

STOCHASTIC ANALYSIS OF THE LINEAR EQUIVALENT RESPONSE OF BRIDGE PIERS WITH ASEISMIC DEVICES

LUISA CARLOTTA PAGNINI*[†] AND GIOVANNI SOLARI[‡]

DISEG, Department of Structural and Geotechnical Engineering, University of Genova, Via Montallegro 1, 16145 Genova, Italy

SUMMARY

The dynamic response of bridge piers with aseismic devices to earthquake excitation is evaluated by the stochastic equivalent linearization technique. The seismic acceleration is schematized through a Gaussian stationary random process. The pier is considered linear elastic, the span is idealized as a rigid mass, the restoring force of the device is represented through a non-linear differential model. The study of the complex modes of the linearized system gives an interpretation of the mechanical behaviour, leads to a formally elementary solution and highlights some phenomena which are typical of the hysteretic systems, particularly of those marked by weak hardening. Even though the solution is limited to the stationary field, it brings out several noteworthy considerations about the effective non stationary behaviour of the structure. Copyright © 1999 John Wiley & Sons, Ltd.

KEY WORDS: aseismic devices; bridge piers; hysteretic systems; non-linear response; stationary analysis; stochastic equivalent linearization

1. INTRODUCTION

The recent research developments in the seismic field and the progress in the technological sector have brought into being a new generation of structures with isolator and/or dissipator devices and a vast scientific literature concerning the analysis of their dynamic response.^{1–3} However, while studies of isolated buildings have covered an ever widening field, even though the isolated bridges are by now very numerous, the specific literature on these structures appears still to be in an embryo stage. Two main distinct approaches can be identified.^{4,5}

The first one is based on finite element analyses, in the non-linear field, in the deterministic time domain.^{6,7} Although this procedure accurately reproduces the mechanics of the system it does not allow interpretations of general nature, nor does it make the physics of some behavioural aspects clear. The setting out of design criteria,⁸ obtained through extended parametric analyses, is strongly limited by the numerical burden of the solution.

*Correspondence to: Luisa Carlotta Pagnini, DISEG, Department of Structural and Geotechnical Engineering, University of Genova, Via Montallegro 1, 16145 Genova, Italy. E-mail: pagnini@diseg.unige.it

[†] Ph.D. Research Assistant

[‡] Professor and Head

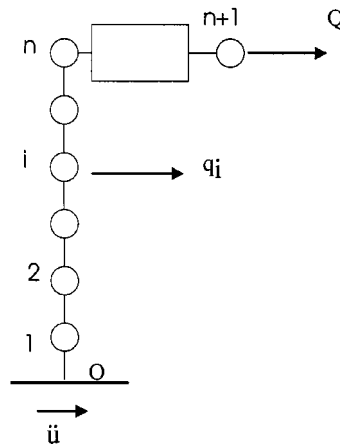


Figure 1. Pier-device-span system

The alternative approach stems from simplified models whose mechanical characteristics are concentrated in few parameters.^{9,10} While representing an extreme schematization of the phenomenon, they are widely regarded for their simplicity and ease. Moreover, they allow analytical representations and advanced solution technique applications.

Operating in the latter context the authors have recently formulated a procedure for the study of the dynamic response of a pier-device-span system subjected to seismic excitation.¹¹ The pier is linear elastic, the restoring force of the aseismic device is represented through a non-linear differential model, the span is schematized as a rigid mass. Applying the modal synthesis, the substructure and the matrix condensation technique, the equations of motion have been formulated in the state variable space. Working in the deterministic time domain, the most appropriate representation models and the effect of the schematization introduced have been studied through extended parametric analyses.

Starting from this study, the present paper evaluates the dynamic response of the structure through the stochastic equivalent linearization. The seismic acceleration is represented as a Gaussian process, the solution of the linearized system is obtained through the covariance technique and the spectral analysis. The study of the natural complex modes gives an effective physical representation and explains the mechanical behaviour of weak hardening hysteretic systems; the analysis, carried out in the stationary field, leads to quite simple analytical solutions without excluding some notable considerations on the effective non-stationary behaviour.¹²

2. NON-LINEAR EQUATIONS OF MOTION

Consider the plane model of the pier-device-span system illustrated in Figure 1.¹¹ The pier, clamped in O in the ground, is linear elastic, axially stiff and is schematized by n masses concentrated in the nodes. The span, connected to the top of the pier through an aseismic device, is idealized by a rigid mass M . Assuming that the system undergoes a seismic horizontal acceleration $\ddot{u}(t)$ applied in O, the matrix condensation technique reduces the degrees of freedom of the problem to the $n + 1$ components of the horizontal nodal displacements.

Let $\mathbf{q}(t) = \{q_1(t)q_2(t) \cdots q_n(t)\}^T$ be the vector, function of time t , which lists the Lagrangian components of the nodal displacements of the pier nodes relative to the ground; $Q(t)$ is the horizontal displacement of the mass M relative to the ground. The restoring force F exerted by the device on the mass M in the Q direction is given by

$$F(t) = -kx(t) - c\dot{x}(t) - f_y z(t) \quad (1)$$

where $x = Q - q_n$, is the relative displacement of the span with respect to the top of the pier; k , c , f_y are, respectively, the post-yield stiffness, the viscous damping coefficient and the plastic threshold of the aseismic device; z is a dimensionless hysteretic component related to x through the following first-order non-linear differential equation:

$$\dot{z}(t) = G(\dot{x}, z, t) \quad (2)$$

The non-linear term in equation (2) can be made explicit by applying Wen's model¹³

$$G(\dot{x}, z, t) = -\gamma \left| \frac{\dot{x}(t)}{x_y} \right| |z(t)|^{\eta-1} - \beta \frac{\dot{x}(t)}{x_y} |z(t)|^{\eta} + \alpha \frac{\dot{x}(t)}{x_y} \quad (3)$$

where α , β , γ , η are non-dimensional parameters which control the hysteresis loop, x_y is a plastic displacement threshold.

The equations of motion constitute a system of $n + 2$ second order, non-linear differential equations, in the $n + 2$ unknowns q_1, \dots, q_n, Q, z :

$$\begin{aligned} & \begin{bmatrix} \mathbf{M} & \mathbf{0} & \mathbf{0} \\ \mathbf{0}^T & M & 0 \\ \mathbf{0}^T & 0 & 0 \end{bmatrix} \begin{Bmatrix} \ddot{\mathbf{q}}(t) \\ \ddot{Q}(t) \\ \ddot{z}(t) \end{Bmatrix} + \begin{bmatrix} \mathbf{C} + c\mathbf{S} & -c\mathbf{v} & \mathbf{0} \\ -c\mathbf{v}^T & c & 0 \\ \mathbf{0}^T & 0 & 1 \end{bmatrix} \begin{Bmatrix} \dot{\mathbf{q}}(t) \\ \dot{Q}(t) \\ \dot{z}(t) \end{Bmatrix} \\ & + \begin{bmatrix} \mathbf{K} + k\mathbf{S} & -k\mathbf{v} & -f_y\mathbf{v} \\ -k\mathbf{v}^T & k & f_y \\ \mathbf{0}^T & 0 & 0 \end{bmatrix} \begin{Bmatrix} \mathbf{q}(t) \\ Q(t) \\ z(t) \end{Bmatrix} - \begin{Bmatrix} \mathbf{0} \\ 0 \\ 1 \end{Bmatrix} G(\dot{Q} - \dot{q}_n, z, t) = - \begin{bmatrix} \mathbf{M} & \mathbf{0} & \mathbf{0} \\ \mathbf{0}^T & M & 0 \\ \mathbf{0}^T & 0 & 0 \end{bmatrix} \begin{Bmatrix} \mathbf{1} \\ 1 \\ 1 \end{Bmatrix} \ddot{u}(t) \quad (4) \end{aligned}$$

in which \mathbf{M} , \mathbf{C} and \mathbf{K} are the $n \times n$ matrices of mass, viscous damping and stiffness of the pier free at the top; $\mathbf{1} = \{1 \dots 1\}^T$, $\mathbf{v} = \{0 \dots 0\}^T$, $\mathbf{0} = \{0 \dots 0\}^T$ are column vectors of n components, $\mathbf{S} = [\mathbf{0} \dots \mathbf{0} \mathbf{v}]$ is an $n \times n$ matrix.

Let $\mathbf{C} = a_0\mathbf{K} + a_1\mathbf{M}$, with a_0 , a_1 be appropriate constants. Applying the modal synthesis technique as discussed by Pagnini *et al.*,¹¹ the transformation:

$$\begin{Bmatrix} \mathbf{q}(t) \\ Q(t) \\ z(t) \end{Bmatrix} = \begin{bmatrix} \Psi & \mathbf{0} & \mathbf{0} \\ \mathbf{v}^T\Psi & 1 & 0 \\ 0 & 0 & 1 \end{bmatrix} \begin{Bmatrix} p(t) \\ x(t) \\ z(t) \end{Bmatrix} \quad (5)$$

is applied where p is the first generalized co-ordinate of the pier and $\Psi = \{\psi_1, \psi_2, \dots, \psi_n\}^T$ is the first eigenvector normalized by the law $\Psi^T\mathbf{M}\Psi = 1$. By virtue of equation (5), equation (4) is

brought back to a system of 3 second-order differential equations in the unknowns p , x , z :

$$\begin{aligned} & \begin{bmatrix} 1 + M(\psi_n)^2 & M\psi_n & 0 \\ M\psi_n & M & 0 \\ 0 & 0 & 0 \end{bmatrix} \begin{Bmatrix} \ddot{p}(t) \\ \ddot{x}(t) \\ \ddot{z}(t) \end{Bmatrix} + \begin{bmatrix} 2\zeta_p\omega_p & 0 & 0 \\ 0 & c & 0 \\ 0 & 0 & 1 \end{bmatrix} \begin{Bmatrix} \dot{p}(t) \\ \dot{x}(t) \\ \dot{z}(t) \end{Bmatrix} \\ & + \begin{bmatrix} \omega_p^2 & 0 & 0 \\ 0 & k & f_y \\ 0 & 0 & 0 \end{bmatrix} \begin{Bmatrix} p(t) \\ x(t) \\ z(t) \end{Bmatrix} - \begin{Bmatrix} 0 \\ 0 \\ 1 \end{Bmatrix} G(\dot{x}, z, t) = - \begin{bmatrix} \sum_{i=1}^n \psi_i m_i & M\psi_n & 0 \\ 0 & M & 0 \\ 0 & 0 & 0 \end{bmatrix} \begin{Bmatrix} 1 \\ 1 \\ 1 \end{Bmatrix} \ddot{u}(t) \end{aligned} \quad (6)$$

where $\omega_p = \sqrt{\Psi^T \mathbf{K} \Psi}$, $\zeta_p = (a_0 \omega_p^2 + a_1)/2\omega_p$ are, respectively, the fundamental circular frequency and the first modal damping coefficient of the pier free at the top.

Operating in the state variable space, equation (6) can be led to a system of five non-linear first-order differential equations in the unknowns p , x , \dot{p} , \dot{x} , z :

$$\dot{\mathbf{x}}(t) = \mathbf{G}\mathbf{x}(t) + \mathbf{r}(t) + \mathbf{p}\ddot{u}(t) \quad (7)$$

where \mathbf{x} is the state variables vector, \mathbf{G} is the dynamic matrix, \mathbf{r} and \mathbf{p} are column vectors which lists, respectively, the non-linear terms and the multiplying coefficients of \ddot{u} :

$$\mathbf{x}(t) = \{p(t) \ x(t) \ \dot{p}(t) \ \dot{x}(t) \ z(t)\}^T \quad (8)$$

$$\mathbf{G} = \begin{bmatrix} 0 & 0 & 1 & 0 & 0 \\ 0 & 0 & 0 & 1 & 0 \\ -\omega_p^2 & k\psi_n & -2\zeta_p\omega_p & c\psi_n & f_y\psi_n \\ \psi_n\omega_p^2 & -\frac{k}{M} - k(\psi_n)^2 & 2\zeta_p\omega_p\psi_n & -\frac{c}{M} - c(\psi_n)^2 & -f_y\frac{1}{M} - f_y(\psi_n)^2 \\ 0 & 0 & 0 & 0 & 0 \end{bmatrix} \quad (9)$$

$$\mathbf{r}(t) = \{0 \ 0 \ 0 \ 0 \ G(\dot{x}, z, t)\}^T \quad (10)$$

$$\mathbf{p} = \left\{ 0 \ 0 \ -\sum_{i=1}^n \psi_i^1 m_i \ \sum_{i=1}^n \psi_n^1 \psi_i^1 m_i - 1 \ 0 \right\}^T \quad (11)$$

Equation (7) is singular for $k = 0$, that is when the device does not exhibit hardening behaviour. The solution of this problem in the deterministic field is discussed by Pagnini *et al.*¹¹

3. STOCHASTIC EQUIVALENT LINEARIZATION

Let us consider the following linear equations of motion:

$$\dot{\mathbf{x}}(t) = (\mathbf{G} + \mathbf{G}_e) \mathbf{x}(t) + \mathbf{p}\ddot{u}(t) \quad (12)$$

$$\mathbf{G}_e = - \begin{bmatrix} 0 & 0 & 0 & 0 & 0 \\ 0 & 0 & 0 & 0 & 0 \\ 0 & 0 & 0 & 0 & 0 \\ 0 & 0 & 0 & 0 & 0 \\ 0 & 0 & 0 & \alpha_e & \beta_e \end{bmatrix} \quad (13)$$

where α_e , β_e are appropriate parameters. In the hypothesis of stationarity, the linear system defined by equation (12) is defined as equivalent¹⁴ to the actual non-linear system (equation (7)) when α_e , β_e minimize the quantity:

$$\Delta = E[\varepsilon^2(t)], \quad \varepsilon(t) = G(\dot{x}, z, t) + \alpha_e \dot{x}(t) + \beta_e z(t) \quad (14)$$

where $E[\cdot]$ is the expectation operator and \dot{x} , z are the solution of the linearized system. Setting the partial derivative of Δ with respect to α_e and β_e equal to zero, a system of two algebraic first order linear equations is obtained whose unknowns, α_e and β_e , are given by:

$$\alpha_e = \frac{-E[G(\dot{x}, z, t) \dot{x}(t)] E[z^2(t)] + E[G(\dot{x}, z, t) z(t)] E[\dot{x}(t) z(t)]}{E[\dot{x}^2(t)] E[z^2(t)] - E[\dot{x}(t) z(t)]^2} \quad (15a)$$

$$\beta_e = \frac{-E[G(\dot{x}, z, t) z(t)] E[\dot{x}^2(t)] + E[G(\dot{x}, z, t) \dot{x}(t)] E[\dot{x}(t) z(t)]}{E[\dot{x}^2(t)] E[z^2(t)] - E[\dot{x}(t) z(t)]^2} \quad (15b)$$

It can be shown that, if α_e and β_e exist so as to satisfy equation (15), then the corresponding value of Δ is not greater than the one associated to any other pair of parameters.¹⁴ Moreover, assuming that the seismic excitation is Gaussian, one has¹⁵:

$$\alpha_e = -E \left[\frac{\partial G(\dot{x}, z, t)}{\partial \dot{x}} \right], \quad \beta_e = -E \left[\frac{\partial G(\dot{x}, z, t)}{\partial z} \right] \quad (16)$$

Representing the non-linear term through Wen's model (equation (3)), the parameters α_e and β_e are obtained in closed form.¹³ In the particular but classical case of $\eta = 1$:

$$\alpha_e = \sqrt{\frac{2}{\pi}} \sigma_z (\gamma \rho_{\dot{x}z} + \beta) - \alpha, \quad \beta_e = \sqrt{\frac{2}{\pi}} \sigma_{\dot{x}} (\gamma + \beta \rho_{\dot{x}z}) \quad (17)$$

where α , β , γ are the parameters of the differential model (equation (3)), $\sigma_{\dot{x}}$, σ_z are the root-mean-square (rms) values of \dot{x} and z , $\rho_{\dot{x}z}$ is the correlation coefficient of \dot{x} , z .

The response of the system is determined by an iterative procedure whose steps contemplate, on one hand, the calculation of α_e , β_e in terms of the linearized response, and, on the other, the solution of linear systems, the first of which is characterized by trial values of α_e and β_e . The solution of each linear system can be obtained through the covariance or the spectral analysis. In both cases the complex modal analysis makes the solution particularly expressive offering an effective characterization of the system's mechanical behaviour.

4. COMPLEX MODAL ANALYSIS

Let:

$$\mathbf{\Lambda} = \text{diag}[\lambda_1, \lambda_2, \dots, \lambda_5], \quad \mathbf{D} = [\mathbf{d}_1 \quad \mathbf{d}_2 \quad \dots \quad \mathbf{d}_5] \quad (18)$$

be square five-order matrices whose terms λ_i, \mathbf{d}_i ($i = 1, \dots, 5$) are, respectively, the eigenvalues and the eigenvectors of the $(\mathbf{G} + \mathbf{G}_e)$ dynamic matrix of the linear system:

$$\mathbf{D}^{-1}(\mathbf{G} + \mathbf{G}_e)\mathbf{D} = \mathbf{\Lambda} \quad (19)$$

If the eigenvalues are real, also the eigenvectors are real. If the eigenvalues are complex, they are two-by-two complex conjugate and the corresponding eigenvectors enjoy the same property. In the case examined, the order of the problem being odd, one eigenvalue, referred to as $\lambda_0 = -\mu_0$, and the corresponding eigenvector, are certainly real. Numerical analyses¹² show that, in the field of real applications, the four remaining eigenvalues and eigenvectors constitute two pairs of complex conjugate quantities corresponding to the two vibration modes of the mechanical system. Having:

$$\lambda_k = -\mu_k + i\nu_k, \quad \bar{\lambda}_k = -\mu_k - i\nu_k \quad (k = 1, 2) \quad (20)$$

where i is the imaginary unit, $\bar{\bullet}$ is the complex conjugate \bullet , μ_k, ν_k are real quantities, the k th circular frequency ω_k and the k th modal damping coefficient ζ_k are given by¹⁶:

$$\omega_k = \sqrt{\mu_k^2 + \nu_k^2}, \quad \zeta_k = \frac{\mu_k}{\omega_k} \quad (21)$$

Always for real applications μ_0, μ_1, μ_2 are positive scalars and the system is stable. Let:

$$\mathbf{x}(t) = \mathbf{D}\mathbf{y}(t) \quad (22)$$

be the complex principal transformation law, where $\mathbf{y}(t) = \{y_1(t)y_2(t) \dots y_5(t)\}^T$ is the vector of the complex modal co-ordinates. Substituting equation (22) into equation (12) one gets¹⁷:

$$\dot{\mathbf{y}}(t) = \mathbf{\Lambda}\mathbf{y}(t) + \mathbf{g}\ddot{u}(t) \quad (23)$$

$$\mathbf{g} = \mathbf{D}^{-1}\mathbf{p} \quad (24)$$

where the four complex eigenvalues and the real eigenvalue guarantee four complex solutions and one real solution y_0 . Applying the Fourier transform of both sides of equation (23) one has:

$$\tilde{\mathbf{y}}(\omega) = \mathbf{H}(\omega)\mathbf{g}\tilde{\ddot{u}}(\omega) \quad (25)$$

in which ω is the circular frequency, $\tilde{\bullet}$ is the operator:

$$\tilde{\bullet}(\omega) = \int_{-\infty}^{\infty} \bullet(t)\exp(-i\omega t)dt \quad (26)$$

$$\mathbf{H}(\omega) = (i\omega\mathbf{I} - \mathbf{\Lambda})^{-1} = \mathbf{diag}[h_1(\omega), h_2(\omega), \dots, h_5(\omega)] \quad (27)$$

$$h_i(\omega) = \frac{1}{i\omega - \lambda_i} \quad (28)$$

where \mathbf{I} is the identity matrix; $h_i(\omega)$ ($i = 1, \dots, 5$) are the complex frequency response functions of the complex modal co-ordinates. Among these, the one corresponding to the real eigenvalue is given as:

$$h_0(\omega) = \frac{1}{i\omega + \mu_0}. \quad (29)$$

It can be seen (Figure 2) that the modulus of h_0 is a decreasing monotone function. It has a maximum in $\omega = 0$ the amplitude of which is inversely proportional to μ_0 . It tends to zero when μ_0 is large; it tends to infinity when the real eigenvalue ($\lambda_0 = \mu_0 = 0$) is nil.

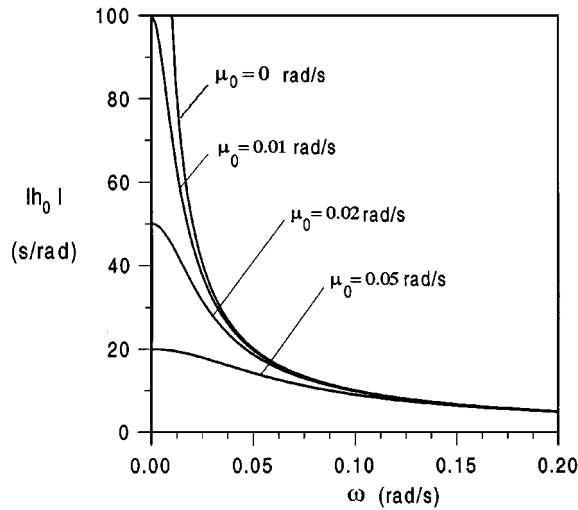


Figure 2. Modulus of the frequency complex response function of the real modal coordinate

The parametric analysis¹² and the following examples show that μ_0 basically depends on the post-yield stiffness k of the device. In particular, it is large when k is large and tends to zero when k tends to zero. In the latter case the matrix $(\mathbf{G} + \mathbf{G}_e)$ is singular; such condition is analogous to the one within the non-linear system.

5. ANALYSIS OF THE LINEARIZED SYSTEM

Let us consider the equation of motion in the space of the complex modal co-ordinates (equation (23)). Since the seismic acceleration $\ddot{u}(t)$ is a zero mean stationary Gaussian random process, the complex modal co-ordinates also constitute zero mean stochastic stationary Gaussian processes. Let \mathbf{V}_y be the covariance matrix of $\mathbf{y}(t)$ at the lag time $\tau = 0$:

$$\mathbf{V}_y = E[\bar{\mathbf{y}}(t)\mathbf{y}^T(t)] \quad (30)$$

The main diagonal terms $(\mathbf{V}_y)_{ii} = E[y_i^2]$ ($i = 1, \dots, 5$) are the variances of the modal co-ordinates; the off-diagonal terms $(\mathbf{V}_y)_{ij} = E[\bar{y}_i y_j]$ ($i, j = 1, \dots, 5; i \neq j$) are the covariances.

In the hypothesis in which the earthquake is a white noise process, its power spectral density function (psdf) is $S_{\ddot{u}}(\omega) = S_0$ and \mathbf{V}_y is given by the equation¹⁴:

$$\bar{\Lambda}\mathbf{V}_y + \mathbf{V}_y\Lambda + 2\pi S_0 \bar{\mathbf{g}}\mathbf{g}^T = \mathbf{O} \quad (31)$$

in which \mathbf{O} is a 5×5 nil term matrix. Being Λ diagonal, equation (31) constitutes a system of 25 independent equations whose solutions are:

$$(\mathbf{V}_y)_{ij} = -\frac{2\pi S_0 \bar{g}_i g_j}{\bar{\lambda}_i + \lambda_j} \quad (i, j = 1, \dots, 5) \quad (32)$$

Since \mathbf{V}_y is a Hermitian matrix the number of the equations and of the unknowns is reduced to 15; taking equally into account the existence of two pairs of complex conjugate solutions, the number of equations and unknowns is in fact 13.

Applying equation (22) the covariance matrix of $\mathbf{x}(t)$ at the lag time $\tau = 0$ is:

$$\mathbf{V}_x = E[\mathbf{x}(t)\mathbf{x}^T(t)] = \bar{\mathbf{D}}\mathbf{V}_y\mathbf{D}^T \quad (33)$$

The extension of the above method to non-white seismic processes is achieved through the prefilters technique.¹⁴ The knowledge of the harmonic content of the response requires, in every case, the solution is sought in the frequency domain.

Let \mathbf{S}_x , \mathbf{S}_y be the cross-power spectral density matrices of \mathbf{x} , \mathbf{y} . On the basis of equation (22)

$$\mathbf{S}_x(\omega) = \bar{\mathbf{D}}\mathbf{S}_y(\omega)\mathbf{D}^T \quad (34)$$

By virtue of equation (25):

$$\mathbf{S}_y(\omega) = \bar{\mathbf{H}}(\omega)\bar{\mathbf{g}}\mathbf{g}^T\mathbf{H}^T(\omega)\mathbf{S}_{ii}(\omega) \quad (35)$$

from which the i , j th term of \mathbf{S}_y can be derived as:

$$[\mathbf{S}_y(\omega)]_{ij} = \frac{\bar{g}_i g_j}{(i\omega - \bar{\lambda}_i)(i\omega - \bar{\lambda}_j)} S_{ii}(\omega) \quad (36)$$

The covariance matrices \mathbf{V}_x , \mathbf{V}_y are obtained by integrating, in the frequency domain, the corresponding spectral matrices:

$$\mathbf{V}_\alpha = \int_{-\infty}^{+\infty} \mathbf{S}_\alpha(\omega) d\omega \quad (\alpha = \mathbf{x}, \mathbf{y}) \quad (37)$$

As will be shown later on, the psdf of the state variables offers essential information for the physical interpretation of this subject.

6. NUMERICAL APPLICATIONS

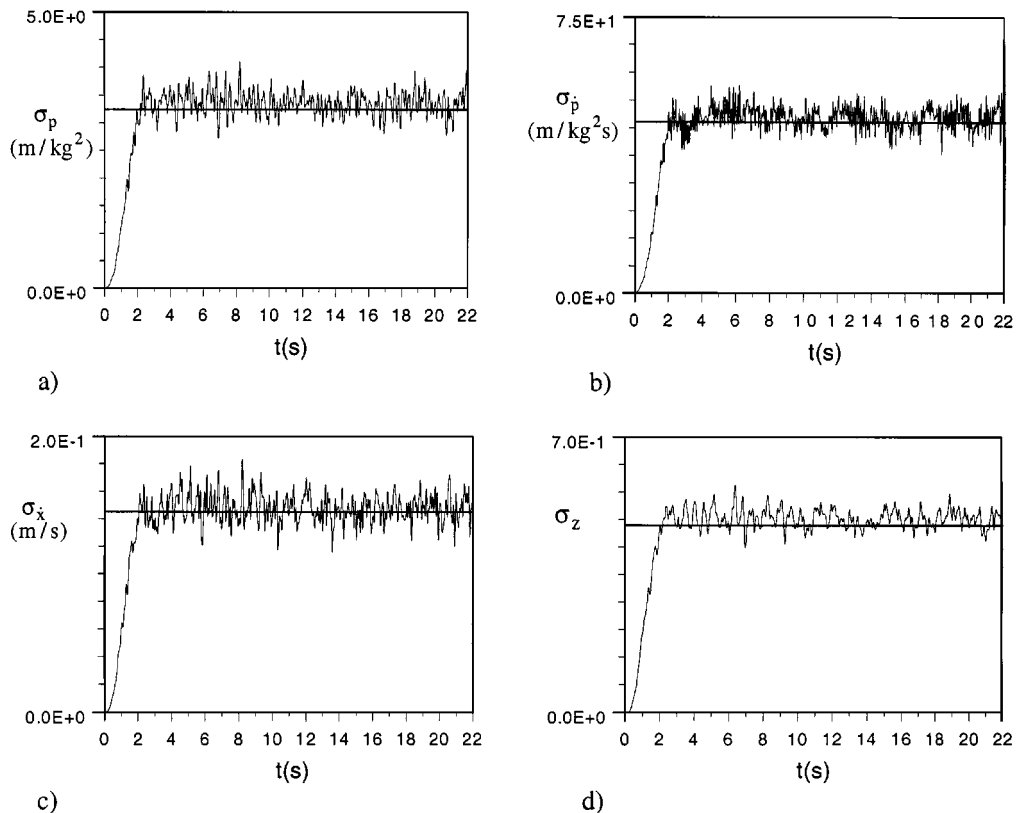
In order to illustrate the effectiveness and the application of the above procedure a pier-device-span system is examined reproducing a portion of the viaduct constructed on a stretch of the Gumusowa-Gerede Anatolic motorway.¹⁸ The height of the pier is $H = 28$ m, its elastic modulus is $E = 2.36 \times 10^{10}$ N/m², its mass density is $\rho = 2.5$ t/m³; the area and the moment of inertia of the section are, respectively, $A = 14.3$ m² and $J = 38.3$ m⁴. Consistently with the model in Figure 1, it is represented as a system with seven nodes placed at constant steps $h_i = H/7$ ($i = 1, \dots, 7$); the nodal masses are $m_i = \rho A h_i$, for $i = 1, \dots, 6$, $m_i = \rho A h_i/2$, for $i = 7$. The circular fundamental frequency of the pier is $\omega_p = 21.9$ rad/s; ξ_p is assumed equal to 5 per cent. The portion of the span considered has mass $M = 1100$ t. The hysteretic restoring force of the device is described through Wen's model (equation 3) assuming $f_y = 1330$ kN, $x_y = 0.025$ m, $\kappa = 1.5$ per cent, κ being the ratio between the post-yield (k) and the pre-yield stiffness (f_y/x_y); $\gamma = 0.9$, $\beta = 0.1$, $\alpha = 1$, $\eta = 1$. The viscous damping of the device is ignored ($c = 0$).

The seismic acceleration process has been modelled through a white noise, $S_{ii}(\omega) = S_0$, a Kanai-Tajimi spectrum,^{19,20} $S_{ii}(\omega) = |H_1(\omega)|^2 S_0$, a Kanai-Tajimi spectrum modified by Clough and Penzien,²¹ $S_{ii}(\omega) = |H_1(\omega)|^2 |H_2(\omega)|^2 S_0$, where:

$$|H_1(\omega)|^2 = \frac{1 + 4\xi_g^2(\omega/\omega_g)^2}{[1 - (\omega/\omega_g)^2]^2 + 4\xi_g^2(\omega/\omega_g)^2}, \quad |H_2(\omega)|^2 = \frac{(\omega/\omega_f)^4}{[1 - (\omega/\omega_f)^2]^2 + 4\xi_f^2(\omega/\omega_f)^2} \quad (38)$$

Table I. Equivalent linearization parameters

| $S_0 \times 10^3$ ($\text{m}^2/\text{rad}/\text{s}^3$) | a/g | α_e (m^{-1}) | β_e (s^{-1}) | λ_0 (rad/s) | ω_1 (rad/s) | ω_2 (rad/s) | ξ_1 (%) | ξ_2 (%) |
|---|-------|-----------------------------------|----------------------------------|--|---|---|----------------|----------------|
| 0.0 | 0.0 | -40.0 | 0 | 0.000 | 102.6 | 9.38 | 0.88 | 2.06 |
| 0.210 | 0.05 | -38.7 | 0.94 | -0.015 | 26.38 | 5.71 | 4.64 | 5.95 |
| 0.840 | 0.1 | -37.44 | 1.66 | -0.026 | 26.23 | 5.65 | 5.07 | 10.2 |
| 8.830 | 0.3 | -32.54 | 4.30 | -0.079 | 25.67 | 5.38 | 6.54 | 28.4 |
| 30.23 | 0.6 | -27.22 | 8.75 | -0.199 | 24.90 | 4.97 | 8.42 | 65.8 |

Figure 3. Rms of: (a) p ; (b) \dot{p} ; (c) \dot{x} , and (d) z for $S_0 = 8.83 \times 10^{-3} \text{ m}^2/\text{rad s}^3$

$\omega_g = 15.6 \text{ rad/s}$, $\omega_f = 1.5 \text{ rad/s}$, $\xi_g = \xi_f = 0.6$ are parameters referred to rocky ground conditions. The results shown in this section refer to the modified Kanai-Tajimi spectrum.

Table I shows the parameters α_e , β_e , the real eigenvalue λ_0 , the natural circular frequencies ω_k and the modal damping coefficients ξ_k ($k = 1, 2$, equation (21)) corresponding to different values of S_0 . The average value of the peak ground acceleration a is calculated on a temporal interval $T = 20 \text{ s}$ by the method proposed by Vanmarke;²² g is the acceleration due to gravity.

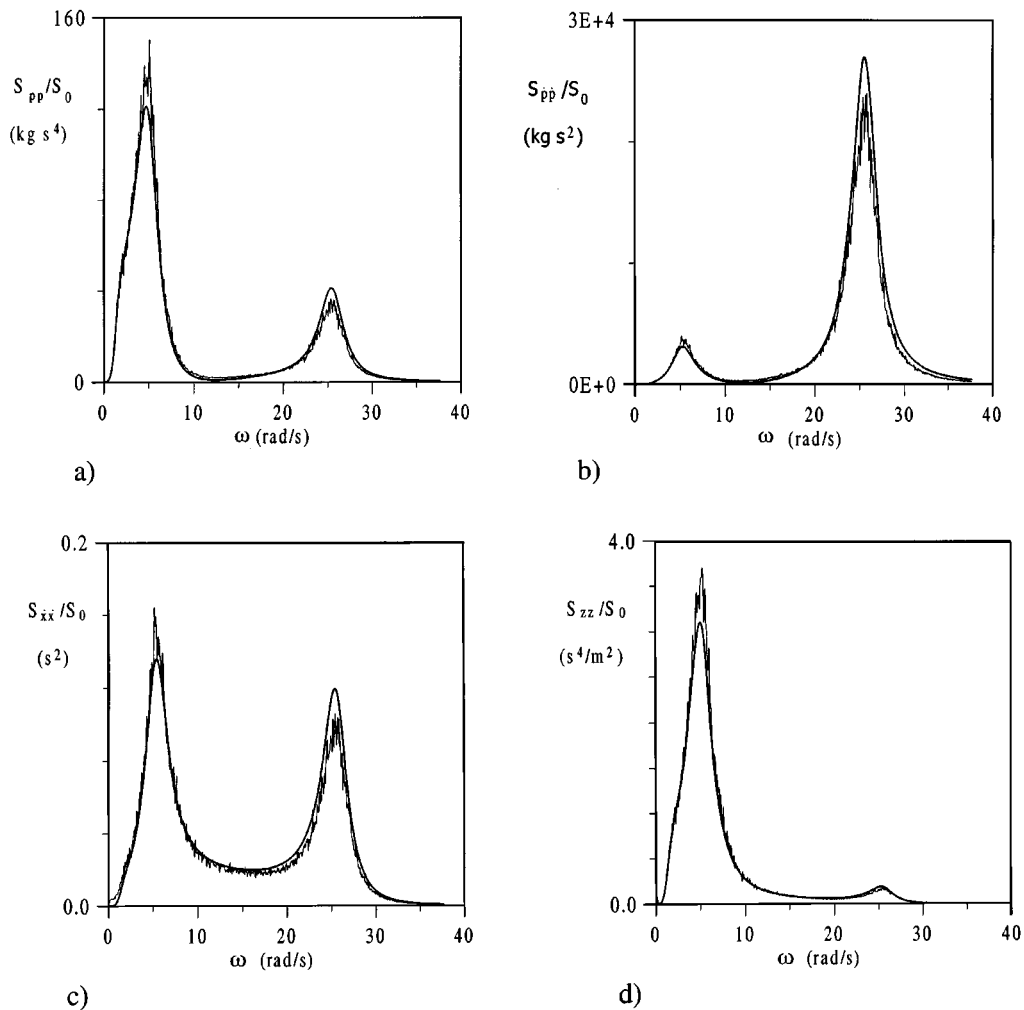


Figure 4. Psdf of: (a) p ; (b) \dot{p} ; (c) \dot{x} ; and (d) z for $\omega > 0$ and $S_0 = 8.83 \times 10^{-3} \text{ m}^2/\text{rad s}^3$

The values in Table I and other parametric analyses¹² show that the decrease of $|\alpha_e|$, tied to the degradation of the stiffness of the device, reduces the natural circular frequencies ω_k ; in particular, for $S_0 = 0$, $\alpha_e = -1/x_y$. The increment of β_e , corresponding to an increase of the hysteretic dissipation, produces an increment of the damping coefficients ξ_k .

The equivalent linear solution (equation (36)) is compared with the results of non-linear analyses (equation (7)) in which the structure is subjected to 100 acceleration time histories, each $T = 22$ s long, with sampling rate $\Delta t = 0.01$ s. They are obtained through a Monte Carlo generation²³ and modulated by a temporal filter (limited to the first 2 s) to minimize the initial transient effects.

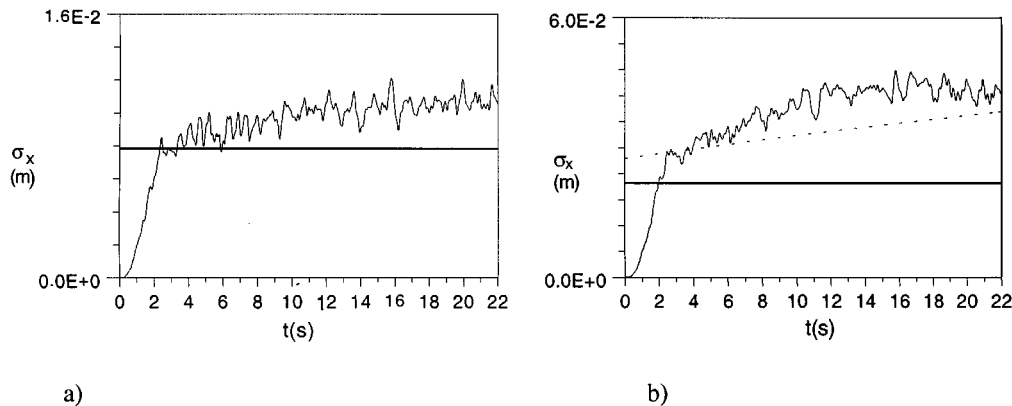


Figure 5. Rms of x for: (a) $S_0 = 0.84 \times 10^{-3}$; and (b) $8.83 \times 10^{-3} \text{ m}^2/\text{rad s}^3$

Figure 3 and 4 show the rms values and the psdf (corresponding to the stationary tract between $t_1 = 2 \text{ s}$ and $t_2 = 22 \text{ s}$) of p, \dot{p}, \dot{x}, z for $S_0 = 8.830 \times 10^{-3} \text{ m}^2/\text{rad s}^3$. The thick lines represent the results of the linear equivalent analysis, the thin lines correspond to the non-linear analysis. Their comparison points out the almost perfect agreement of the results; the approximation is excellent independently of the seismic acceleration level.¹² The spectral analysis also shows up two relative maxima in correspondence with the natural circular frequencies ω_1 and ω_2 . Instead, the harmonic content in $\omega = 0$, tied to the real autovalue λ_0 , is absent; this is also true when the excitation is a white noise and $S_{ii} \neq 0$ for $\omega = 0$ ¹².

Figure 5 shows the rms value of x for $S_0 = 0.84 \times 10^{-3}$ and $8.83 \times 10^{-3} \text{ m}^2/\text{rad s}^3$. Confirming similar results obtained by Iwan and Paparizos²⁴ and by Park,²⁵ the equivalent linear analysis provides underestimates of the displacements given by the non-linear analysis which increase in time and with the seismic intensity.

Park²⁵ attributed this phenomenon to the loss of Gaussianity and of stationarity of the non-linear response. The first gives rise to a generic underestimate of σ_x , the second is associated with the accumulation of plastic deformation and produces an increase in time of σ_x . The author gave an empirical criterion for the correction of the error. Figure 5(b) shows the corrected estimate as a dashed line; corrections for $\sigma_x/x_y < 0.5$ do not apply (Figure 5(a)).

7. THE MOTION OF THE DEVICE

Although the correction technique given by Park leads to reasonably good approximations, it can be observed that, if the excitation is stationary, the non-linear operator is skew-symmetrical and the system is dynamically stable, also the response is stationary. The diagrams in Figure 5 must therefore represent the initial transient of the response.

Figure 6 provides the diagrams of σ_x already shown in Figure 5, now obtained by applying seismic accelerograms of duration $T = 102 \text{ s}$. Figure 7 gives analogous results inherent to white noise excitations with $S_0 = 1.80 \times 10^{-4}$ and $16.1 \times 10^{-4} \text{ m}^2/\text{rad s}^3$. They show that the response process asymptotically tends towards stationarity along with the increase in the time; this trend is

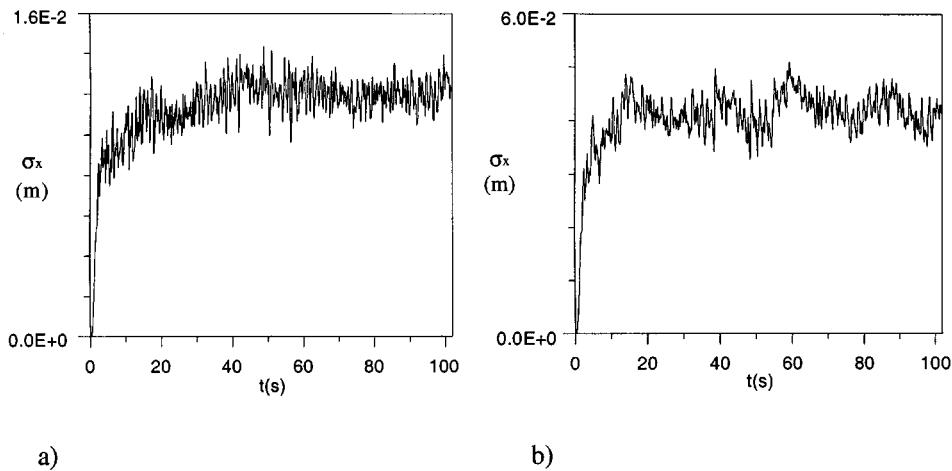


Figure 6. Rms of x for: (a) $S_0 = 0.84 \times 10^{-3}$; and (b) $8.83 \times 10^{-3} \text{ m}^2/\text{rad s}^3$

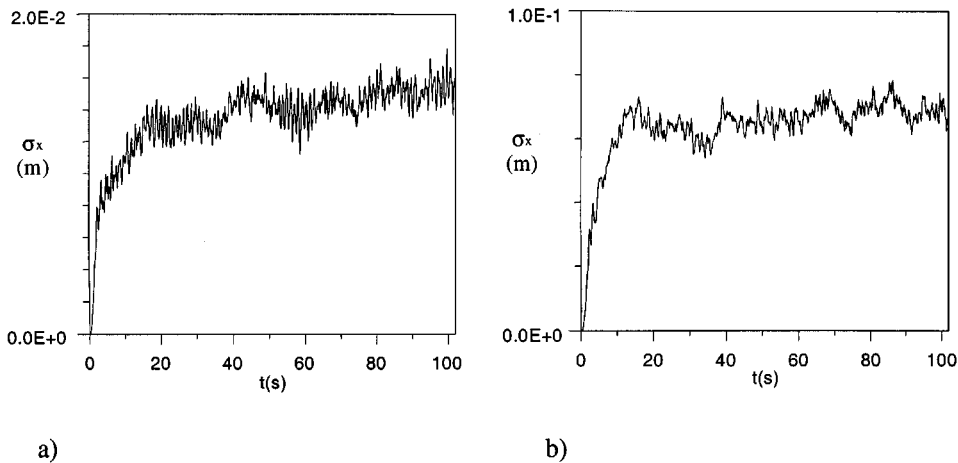


Figure 7. Rms of x for a white noise excitation and: (a) $S_0 = 1.80 \times 10^{-4}$; and (b) $16.1 \times 10^{-4} \text{ m}^2/\text{rad s}^3$

all the more rapid as the excitation becomes more intense and the spectral content of the earthquake is reduced at the low frequencies.

Figures 8 and 9 show the psdf inherent to the case studied above (Figures 6 and 7). The psdf is calculated in the $\bar{T} = 70 \text{ s}$ interval ranging from $t_1 = 32 \text{ s}$ to $t_2 = 102 \text{ s}$ in which the stationary regime is tendentiously reached. The thin line corresponds to the non-linear analysis, the thick line corresponds to the equivalent linear analysis. With the sole exception of the harmonic frequencies close to zero, there is an almost complete overlapping between the different solutions.

The situation changes around $\omega = 0$. The equivalent linear analysis gives spectral values $S_x(0) = 0$ when $S_{ii}(0) = 0$. The non-linear solution produces a low-frequency peak whatever the

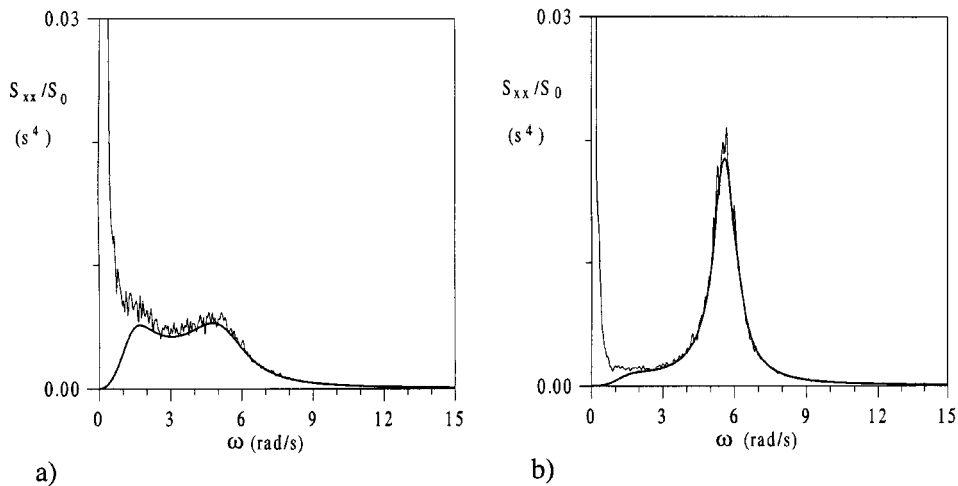


Figure 8. Psdf of x for a modified Tajimi spectrum for: (a) $S_0 = 0.84 \times 10^{-3} \text{ s}$; and (b) $8.83 \times 10^{-3} \text{ m}^2/\text{rad s}^3$

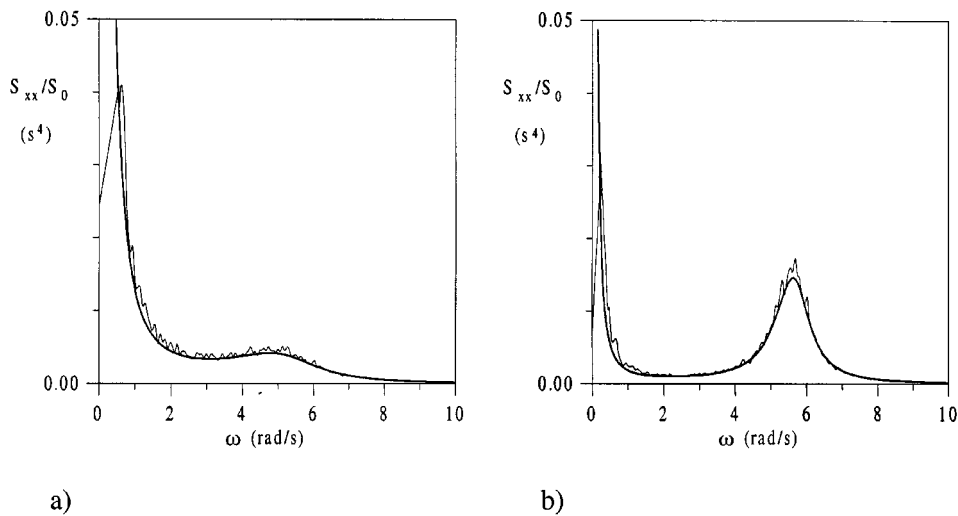


Figure 9. Psdf of x for a white noise spectrum for: (a) 1.80×10^{-4} ; and (b) $16.1 \times 10^{-4} \text{ m}^2/\text{rad s}^3$

spectral content of the earthquake is. This peak can be associated with the physical phenomenon which, in the linearized ambit, gives place to the real eigenvalue and to the peak of $|h_0|$ in $\omega = 0$.

The carrying out of extended parametric analyses¹² demonstrates the generality of these observations and suggests attributing the following expression to the psdf of x around $\omega = 0$:

$$S_{xx}^0(\omega, \bar{T}) = \varphi^2 |h_0(\omega)|^2 \chi^2(\omega, \bar{T}) \quad (39)$$

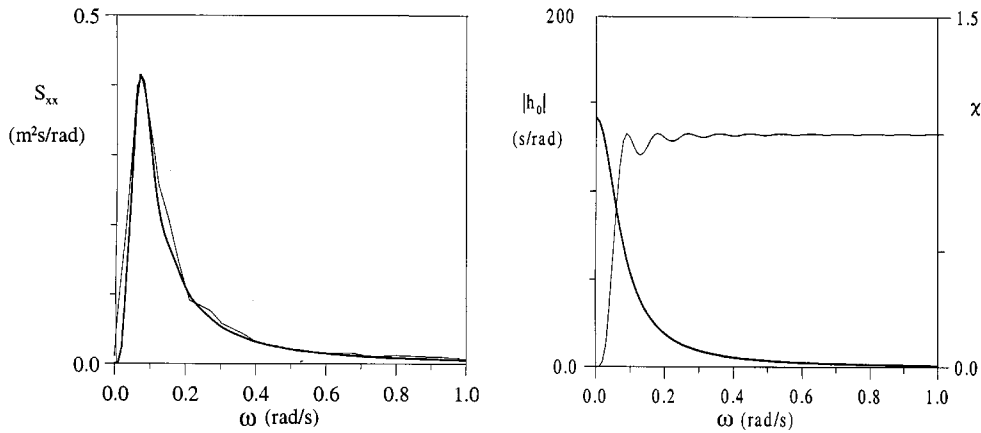


Figure 10. Psdf of x for a modified Tajimi spectrum in: (a) $\omega \approx 0$; and (b) role of $|h_0|$ and χ

where φ is a coefficient which depends on the non-linearity and is nil when the response is linear elastic; χ is a frequency filter eliding the harmonic contents with $\omega < 2\pi/\bar{T}^{26}$:

$$\chi(\Delta t, \bar{T}, \omega) = 1 - \frac{\sin^2(\omega \bar{T}/2)}{(\omega \bar{T}/2)^2} \quad (40)$$

When \bar{T} tends to zero, then $\chi = 0$ and $S_{xx}^0 = 0$. When \bar{T} tends to infinity, then $S_{xx}^0 = \varphi^2 |h_0|^2$.

With reference to the solution in Figure 8, Figure 10(a) shows the psdf of x in correspondence with the frequencies close to zero; the thin line is the results of the non-linear analysis, the thick line corresponds to equation (39) for $\varphi = 0.065 \text{ m/(rad/s)}^{0.5}$. Figure 10(b) shows the role of $|h_0|$ (thick line) and χ (thin line).

In the light of the above observations, the psdf of the asymptotic response of the device can be assumed to be the sum of two contributions:

$$\bar{S}_{xx}(\omega) = S'_{xx}(\omega) + S_{xx}^0(\omega) \quad (41)$$

where S'_{xx} is the psdf of x outside the frequencies close to zero, $S_{xx}^0 = S_{xx}^0(\omega, \infty)$. By virtue of equation (41), the variance of the asymptotic process is expressed by the formulae:

$$\bar{\sigma}_x^2 = (\sigma'_x)^2 + (\sigma_x^0)^2 \quad (42)$$

$$(\sigma'_x)^2 = \int_{-\infty}^{+\infty} S'_{xx}(\omega) d\omega \quad (43)$$

$$(\sigma_x^0)^2 = \int_{-\infty}^{+\infty} S_{xx}^0(\omega) d\omega = -\frac{\pi \varphi^2}{\lambda_0} \quad (44)$$

The rms value of the response of the device at the generic time varies therefore between two limit values. The first, σ'_x , ideally corresponds to an earthquake so short that it does not excite the harmonic frequencies close to zero; it can be determined by resolving the equivalent linear system in the space of the complex modal co-ordinates, ignoring the contribution of the real solution y_0 .

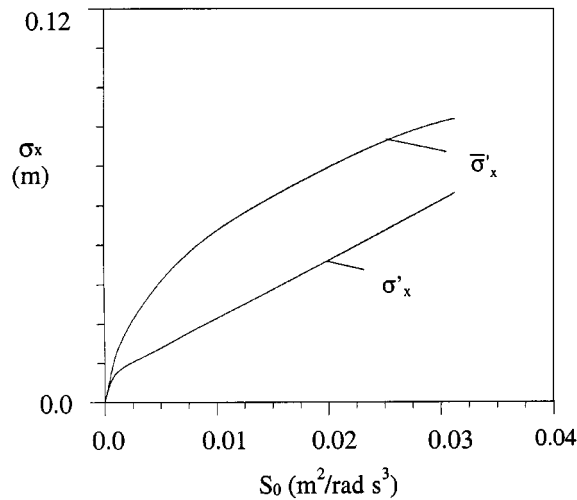
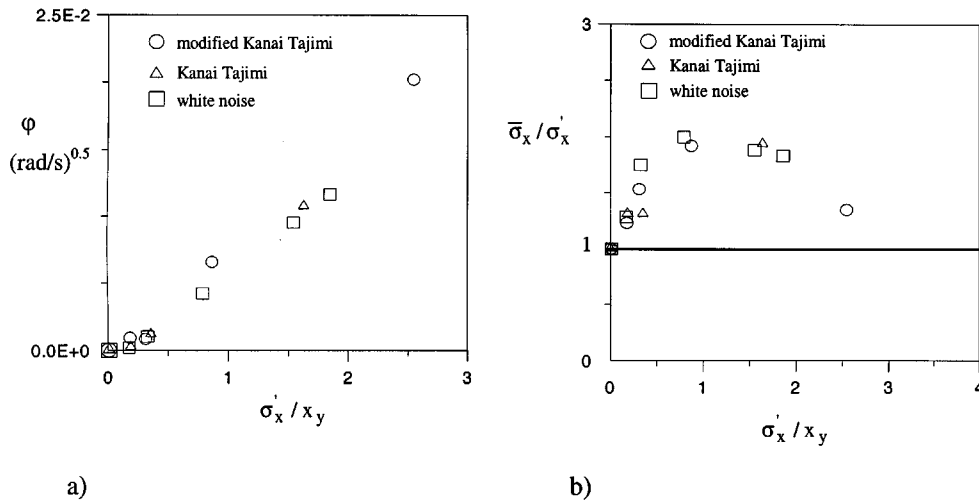


Figure 11. Limit values of the device response

Figure 12. Response of the device (a) ϕ coefficient; (b) stationary response

The second, $\bar{\sigma}_x$, is the stationary value to which the response to earthquakes of infinite duration tends. Figure 11 shows $\bar{\sigma}_x$, σ'_x in terms of S_0 for a modified Tajimi spectrum.

Figure 12 shows ϕ and $\bar{\sigma}_x/\sigma'_x$ in terms of the ratio σ'_x/x_y considered as representative of the non-linearity level. The diagrams are obtained by varying the spectral content of the excitation (white noise, Tajimi spectrum, modified Tajimi spectrum) and the intensity of the seismic acceleration; S_0 varies between 0 and $0.0302 \text{ m}^2/\text{rad s}^3$.

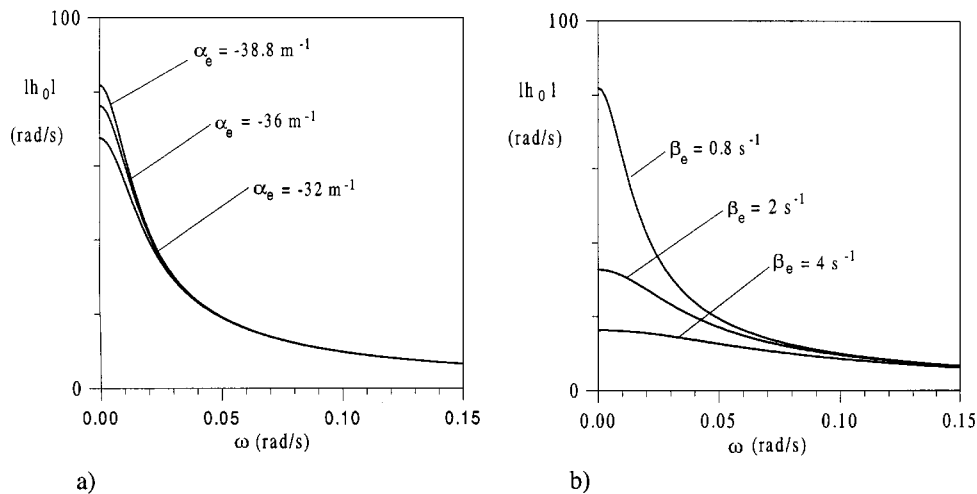


Figure 13. Frequency response function of the modal real coordinate on varying: (a) α_e ; and (b) β_e

These results, although preliminary, seem to be quite interesting. They show that the laws that express φ and $\bar{\sigma}_x/\sigma'_x$ in terms of σ'_x/x_y are almost independent of the spectral content of the excitation and implicitly depend on the seismic intensity through σ'_x/x_y . For $\sigma'_x/x_y = 0$, then $\varphi = 0$ and $\bar{\sigma}_x/\sigma'_x = 1$. As σ'_x/x_y increases, φ grows almost linearly; on the other hand $\bar{\sigma}_x/\sigma'_x$, initially increases, then asymptotically decreases to 1 for σ'_x/x_y tending to infinity.

The decreasing slope in Figure 12 is explained observing that $|h_0|$ tends to zero when $|\alpha_e|$ decreases (Figure 13(a)) and β_e increases (Figure 13(b)). This corresponds to the growth of the seismic intensity (Table I) and therefore to the increase in the non-linearity.

Finally, since $|\lambda_0|$ increases with the post-yield stiffness k of the device, the existence of the hardening slope determines the fall of $|h_0|$ and σ_x^0 , this eliminating the underestimate of the laws of motion $x(t)$. The error of the equivalent linear analysis is already negligible for $\kappa \geq 5$ per cent¹². This condition unfortunately does not correspond to the constructive reality, since such devices are generally characterized by much smaller κ values.

8. CONCLUSIONS

The present paper establishes a dynamical model of a pier-device-span system subjected to seismic motion. Assuming that the seismic excitation is a stochastic Gaussian process, the equivalent linearization technique, applied at this time in the stationary field, gives immediate and precise results as regards the pier response. On the other hand, it cannot reproduce accurately the motion of devices characterized by a very low hardening ratio.

The equations of motion of the hysteretic device are studied applying the complex modal analysis and the spectral analysis. The linearized system has a real eigenvalue to which is associated a harmonic content of the response with frequencies close to zero. The asymptotic response of the device in the non-linear field is the sum of two different contributions which correspond, respectively, to earthquakes of nil and infinite duration. The first is independent of

the real eigenvalue. The second corresponding to the harmonics of the response at low frequency, is associated with the real eigenvalue and depends on the non-linearity level.

Preliminary results suggest that the variability range of the effective response is almost independent of the spectral content of the excitation. The transition from the minimum to the maximum value depends instead on the duration of the input motion, according to laws that will require further analyses. A rigorous and systematic study cannot be performed without a dynamic stochastic analysis in the non stationary and nonlinear field.

ACKNOWLEDGEMENTS

The authors gratefully acknowledge the support of the Gruppo Nazionale per la Difesa dei Terremoti (GNDT) of the National Research Council (CNR) under the grant n° 90CT96 02967.54/115.19644 for the work reported in this paper.

REFERENCES

1. J. M. Kelly, 'Aseismic base isolation: review and bibliography', *Soil Dyn. Earthquake Engng.* **5**(3), 202–216 (1986).
2. R. I. Skinner, W. H. Robinson and G. H. McVerry, *An Introduction to Seismic Isolation*, Wiley, Chichester, 1993.
3. J. M. Kelly, *Earthquake Resistant Design with Rubber*, Springer, London, 1994.
4. M. J. N. Priestley, F. Seible and G. M. Calvi, *Seismic Design and Retrofit of Bridges*, Wiley, New York, 1996.
5. G. M. Calvi and P. Pinto (eds), 'Experimental and numerical investigations on the seismic response of bridges and recommendations for code provisions', European Consortium of Earthquake Shaking Tables, Prenormative Research in Support of Eurocode 8, *Report No. 4*, November 96.
6. H. M. Ali and A. M. Abdel Ghaffar, 'Seismic energy dissipation for cabled stayed bridges using passive devices', *Earthquake Engng. Struct. Dyn.* **23**, 877–893 (1994).
7. J. S. Hwang, J. M. Chiou, L. H. Sheng and J. H. Gates, 'A refined model for base-isolated bridges with bi-linear hysteretic bearings', *Earthquake Spectra* **12**(2), 245–273 (1996).
8. R. W. G. Blakeley, L. G. Cormack and M. J. Stockwell, 'Seismic Design of bridges, section 6, mechanical energy dissipating devices', *Bull. New Zealand Natl. Soc. Earthquake Engng.* **13**(3), 264–268 (1980).
9. M. Dolce, 'A design method for isolation systems of simply supported girder bridges', *Int. Meeting on Base Isolation and Passive Energy Dissipation*, Assisi, 1989.
10. L. Xiaoming, 'Optimization of the stochastic response of a bridge isolation system with hysteretic dampers', *Earthquake Engng. Struct. Dyn.* **18**, 951–964 (1989).
11. L. C. Pagnini, G. Ballio and G. Solari, 'Modeling and nonlinear seismic analysis of bridges with aseismic devices', *European Earthquake Engng.* (1998), press.
12. L. C. Pagnini, *The dynamic Response to Seismic Action of Bridge Piers with Aseismic Devices*, Ph.D. Dissertation, Bologna, 1996 (in Italian).
13. Y. K. Wen, 'Equivalent linearization for hysteretic systems under random excitation', *Trans. ASME* **47**, 150–154 (1980).
14. J. B. Roberts and P. D. Spanos, *Random Vibration and Statistical Linearization*, Wiley, Chichester, 1990.
15. I. E. Kazakov, 'Generalization of the method of statistical linearization to multidimensional systems', *Auto Remote Control* **26**, 458–464 (1965).
16. A. S. Veletsos and C. Ventura, 'Modal analysis of non-classically damped linear systems', *Earthquake Engng. Struct. Dyn.* **14**, 217–243 (1986).
17. K. A. Foss, 'Coordinates which uncouple the equations of motion of damped linear dynamic systems', *J. Appl. Mech. ASME* **25**, 361–364 (1958).
18. Marioni, 'Development of a new type of energy dissipating device for seismic protection of bridges', *Proc. 1st European Conf. on Earthquake Engineering*, Balkema, Rotterdam, 1995, pp. 745–750.
19. K. Kanai, 'Semi-empirical formula for the seismic characteristics of the ground', *Bull. Earthquake Res. Inst. Univ. Tokyo* **35**, 307–325 (1957).
20. H. Tajimi, 'A statistical method of determining the maximum response of a building structure during an earthquake', *Proc. 2nd world Conf. on Earthquake Engng.*, Vol. 2, Tokyo, Japan, 1960, pp. 781–796.
21. R. W. Clough and J. Penzien, *Dynamics of Structures*, McGraw-Hill, New York, 1975.

22. E. H. Vanmarke, 'On the distribution of the first-passage time for normal stationary random process', *J. Appl. Mech.* **3**, 215–220 (1975).
23. M. Shinozuka, 'Monte Carlo solution of structural dynamics', *Comp. Struct.* **2**, 855–874 (1972).
24. W. D. Iwan and L. G. Paparizos, 'The stochastic response of strongly yielding systems', *Prob. Engng. Mech.* **3**(2), 75–82 (1988).
25. Y. J. Park, 'Equivalent linearization for seismic responses. I: formulation and error analysis', *J. Engng. Mech.* **118**(11), 2207–2226 (1992).
26. Strong winds in the atmospheric boundary layer. Part 2: discrete gust speeds, *ESDU 83045*; Engineering Science Data Unit, London, England, 1984.